STUDIA UNIVERSITATIS BABEŞ-BOLYAI, CHEMIA, LIV, 4, 2009

PHYSICO-CHEMICAL CHARACTERIZATION OF 8YSZ NANOPARTICLES BY MODIFIED SOL-GEL METHOD

C. SUCIU[a,b], A. VIK[a], F. GOGA[b], E. DOROLTI[c], R. TETEAN[c], A.C. HOFFMANN[d]

ABSTRACT. 8 mol% Yttria Stabilized Zirconia (8YSZ) powders have been obtained by the modified sol-gel method using sucrose and pectin as organic precursors. The influence of the amounts of both sucrose and pectin were studied experimentally over a range of calcination temperatures. The obtained gels were investigated by Thermogravimetric/Differential Thermal Analysis (TG/DTA) to identify physico-chemical processes that take place during the process and to establish an optimal calcination temperature diagram. The final powders were investigated by X-ray diffraction (XRD) and Transmission Electron Microscopy (TEM) to evaluate the phase composition, the microstructure and morphology. Crystallite size and particle size of the final powders were determined using Scherrer formula and nitrogen adsorption with the Brunauer–Emmett–Teller (BET) isotherm. The results confirm that the particle properties, size and crystallite size, are strongly dependent on the calcination temperature. On the other hand, the particle properties are rather—but not completely—insensitive to (and therefore the process rather "forgiving" for) variations in the amounts of sucrose or pectin used.

Keywords: YSZ, yttria stabilized zirconia, nanoparticles, sol-gel processing, calcination temperature, organic precursors, sucrose, pectin

INTRODUCTION

The sol-gel method is emerging as a low-cost, flexible method for creating nanoparticles, and is also a promising method for creating thin layers of a controlled porosity [1], although much still remains to be known about the influence of the processing parameters on the final product. The method has been used to synthesize nano-sized particles of various materials, such as NiO, TiO_2, ZrO_2, YSZ (yttria-doped zirconia), La_2O_3, CeO_2, $BaFe_{12}O_{19}$ etc., useful for their mechanical, magnetic, ion conducting or optical properties.

[a] *CMR-PROTOTECH AS, NO-5892 Bergen, Norway, crina@prototech.no*
[b] *Universitatea Babeş-Bolyai, Facultatea de Chimie şi Inginerie Chimică, Str. Arany Janos, Nr. 11, RO-400028 Cluj-Napoca, Romania*
[c] *Universitatea Babeş-Bolyai, Faculatea de Fizică, Str. Kogălniceanu, Nr. 1, RO-400084 Cluj-Napoca, Romania*
[d] *University of Bergen, Institute of Physics and Technology, Allegaten 55, 5007 Bergen, Norway*

In what follows we mention some recent studies aimed at determining the effect of processing parameters on the properties of particles synthesized by sol-gel methods utilizing organic precursors, which are subsequently burnt off in a calcination step.

Most authors found a significant influence of the temperature used in the calcination step on the particles size. Increasing the calcination temperature leads to the formation of larger particles as measured by nitrogen adsorption and by TEM, for instance for YSZ particles [2,3]. Wang et al. [4] looked particularly closely at this issue, and found by TEM analysis that the size of La_2O_3 particles increased not only with temperature, but also with the duration of calcination.

A higher calcination temperature also leads to a higher quality of crystallization. In general, higher calcination temperatures give rise to higher and sharper peaks in XRD profiles. Zhang et al. [2] found this for YSZ, as did Laberty-Robert et al. [3]. The latter workers found diffraction peaks characteristic of a tetragonal crystal structure for calcination temperatures below 600^0C, and only a cubic structure above that temperature; they used 8% of Y_2O_3 dopant. Wang et al. [4] found some chemical transformations at lower calcination temperatures, and did not obtain the pattern characteristic for La_2O_3 until 750^0C, with the XRD diffraction pattern becoming much clearer with sharper peaks at 850^0C. Lian et al. [5] prepared a mixture of NiO and doped CeO_2 particles for use in anodes in SOFCs. They also found that the particles are sintering further after their autocombustion manufacturing process. Related to the higher and sharper XRD peaks is the fact that the Scherrer formula indicates larger crystallites for higher calcination temperatures for various types of particles and manufacturing processes [2,5,6]. Jung et al. [7] found that the photoluminescence intensity of their titania particles was enhanced and that the peak position in the photoluminescence spectrum moved to smaller wavelengths, as the calcination temperature was raised. This was all attributed to a progressively more ordered crystalline structure.

Widoniak et al. [8] carried out a special study in this respect. They produced larger TiO_2 and ZrO_2 particles by aggregation of nanoparticles. These particles were sometimes made porous by the judicious addition of different types of salts and polymers to the reaction mixtures. They found crystallite sizes much smaller than their particle sizes, and also much higher specific areas (up to 300 m^3/g) than the particle size would indicate.

Laberty-Robert et al. [9] studied the influence of the precursor ratios for Pechini synthesis of YSZ particles. They did not find a strong variation in the particle properties when varying the ratios citric acid/ethylene glycol or citric acid/transition metal, although they did find large differences in the viscosity of the gels. They attempted to control the particle size by adding surfactant to the reaction mixture to obtain a colloidal suspension, and found decreasing particle size with increasing surfactant concentration. For their strongly agglomerated particles, the BET surface was less than expected from the particle size, as determined by electron microscopy.

Many investigations [2,4,5,6,8] also include thermal analyses of the polymeric gel as it is being heated in a controlled temperature calcination process. In general, it is possible to recognize endothermic processes corresponding to dewatering and exothermic processes corresponding to combustion of organic material. Also exothermic processes corresponding to solid solutions or crystallographic changes can also be observed.

The objective of this work was to use the new modified sol-gel method, with sucrose and pectin as organic precursors, in order to obtain 8YSZ nanoparticles. The effect of the mass ratio between sucrose and pectin on the obtained powders was investigated at a larger domain compared with our previously work [10]. The obtained powders were calcinated at different temperatures and different thermal treatments (see below) to study the influence of the calcination process.

RESULTS AND DISCUSSION

The TA analysis for the A set (Figure 1) revealed an endothermic process at 200^{0}C (for A1) and 180^{0}C (for A4), visible on the DTA curve with a slight mass loss due to water elimination, followed by a large exothermic process visible extended up to 940^{0}C. Oxidation of the organic compound and formation of cubic zirconia stabilized with yttria take place in this large temperature interval and they may overlap.

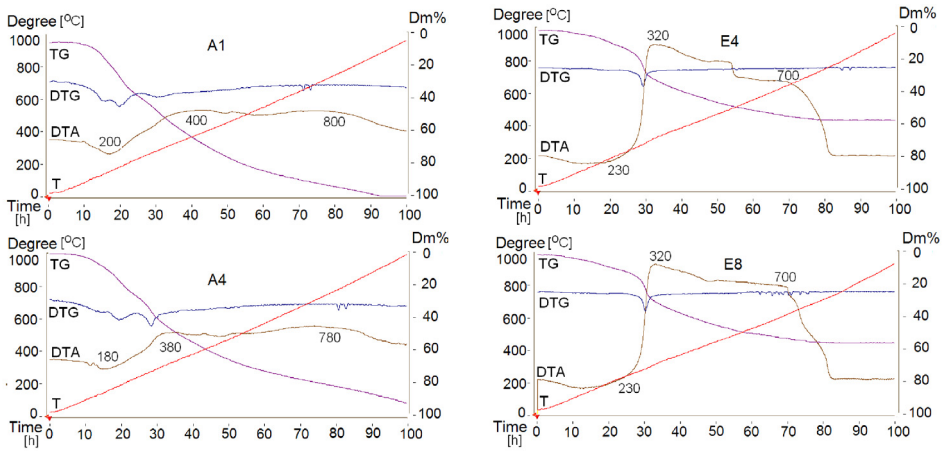

Figure 1. The thermal analysis of the dried gels.

These processes are distinguishable on the DTA curve through the two maxima at 400^{0}C and 780^{0}C (for A1) and at 380^{0}C and 800^{0}C (for A4), respectively. Loss of mass takes place along the whole temperature range from 100 to 940^{0}C, due to the elimination of water vapor and gaseous reaction products, and goes up to 98%.

Turning now to the E set shown in Figure 1, an exothermic peak of high intensity can be observed on the DTA curve. This starts at 230^{0}C and continues up to 840^{0}C. The curves present a maximum at 320^{0}C which corresponds to the oxidation of the organic components followed by a second maximum at around 700^{0}C due to the formation of cubic zirconia. A slight mass loss can be noticed under 200^{0}C on the TG curve due to water elimination. The rate of this process was very low so that no endothermic peak can be distinguished on the DTA curve. The mass loss increased between 230 and 700^{0}C. Overall, a 58% mass loss was determined.

Comparing the two sample sets the following remarks can be made:

– the exothermic effect corresponding to the oxidation of the organic compound was much more intense for the E set, due to the larger amount of organic compound present;

– the total mass variation was higher for the A set (98%) compared to the E set (58%), likely due to the higher water retention in the A set. Also, the gas elimination was slower along the whole temperature interval;

– the strong endothermic process in the A samples under 200^{0}C shows that more residual water was present in these samples. Thus the procedure of obtaining the A set yielded gels which retained water and gasses more strongly, and their elimination was more difficult and required higher temperatures;

– the exothermic effect corresponding to the formation of cubic zirconia was much more intense for the E set and ended at 840^{0}C. In the A set this process was much less intense, and persisted up to higher temperatures (940^{0}C). This shows that the crystallization process into cubic zirconia had a lower rate for the A set.

The obtained BET values of the specific surface area (S), the pore volumes (V_P) and the BJH pore diameter (r_p) for all the samples, at different sintered temperatures, are shown in the Figure 2.

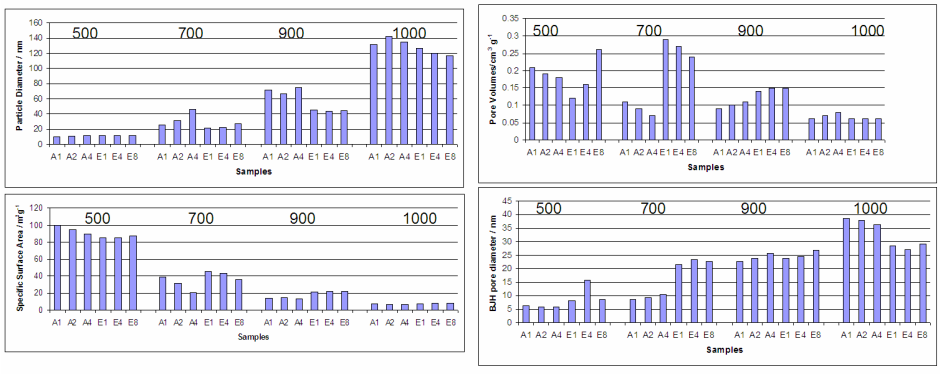

Figure 2. Specific surface area, pore volumes, BJH pore diameter and nanoparticles diameter at different temperatures.

Assuming that the particles are round and the theoretical density (ρ) of 8mol% YSZ is 6100 kg/m^3 [12], the equivalent grain size (D) corresponding to the obtained specific surface areas (S) were calculated following equation: $D=6/(\rho \cdot S)$.

Specific surface area decreased with the increasing of the calcination temperature. For example, the samples calcined at 500^{0}C have the highest specific surface area. However, upon calcination at 1000^{0}C, the specific surface area of the samples is reduced. This seems to be mostly due to the reduction in bulk porosity of the compound. On the other hand it is somewhat insensitive to the amount - and the proportions - of the organic precursors used. The highest specific area of 99.9 m^2/g was obtained at 500^{0}C and the values decreased with increasing temperature down to 6.9 m^2/g at 1000^{0}C.

The mean particle diameter decreased by increasing the temperature and by decreasing specific surface area. The values of the mean particle sizes vary from ~10 nm (500^{0}C) to ~150 nm (1000^{0}C). In the same way, the BJH pore diameters increased by increasing the temperature showing the presence of mesopores (smaller that 40 nm) even for the samples calcined at high temperatures.

Specific pore volume is calculated as the sum of volumes of all pores in one gram of adsorbent. We have to emphasise that for our samples, only internal volume inside the adsorbent particles was counted. At low calcination temperatures (500-700^{0}C), the obtained powders exhibit an increased pore volume, while, as the calcination temperatures increase (900-1000^{0}C), the pore volume decreased. This is mainly due to the longer thermal process, which allows the particles to grow in dimension and the pores to close.

The XRD data from all the samples show the presence of only one single phase, solid solution of ZrO_2 with Y_2O_3. The pattern no. 49-1468 corresponds to Yttrium Zirconium Oxide - $Y_{0.15}Zr_{0.85}O_{1.93}$–$92ZrO_28Y_2O_3$. The presences of other phases were not observed. Based on the phases identified in the XRD patterns, it can be concluded that a homogeneous solid solution of ZrO_2 with Y_2O_3, necessary to form cubic zirconia, was formed (Figure 3). The XRD of the mixtures treated at low temperature (500^{0}C) show a significant difference between the E and the A sets due to the mass ratio of sucrose:pectin used in the experiments. The spectra of the E set, obtained with a smaller amount of pectin, are sharper with relatively less noise, due to a better crystallization. At higher temperatures (700-1000^{0}C) the differences between the shapes of the peaks are less noticeable.

The FWHM and the 2θ values of the first four peaks were used to calculate the crystallite sizes of the obtained powders at different temperatures using the Scherrer formula [13]. In Figure 4 the mean crystallite size for all samples at each temperature in the studied interval are shown. The mean crystallite sizes varied between ~6 and 37 nm showing that the method is effective to synthesize nanosized powders.

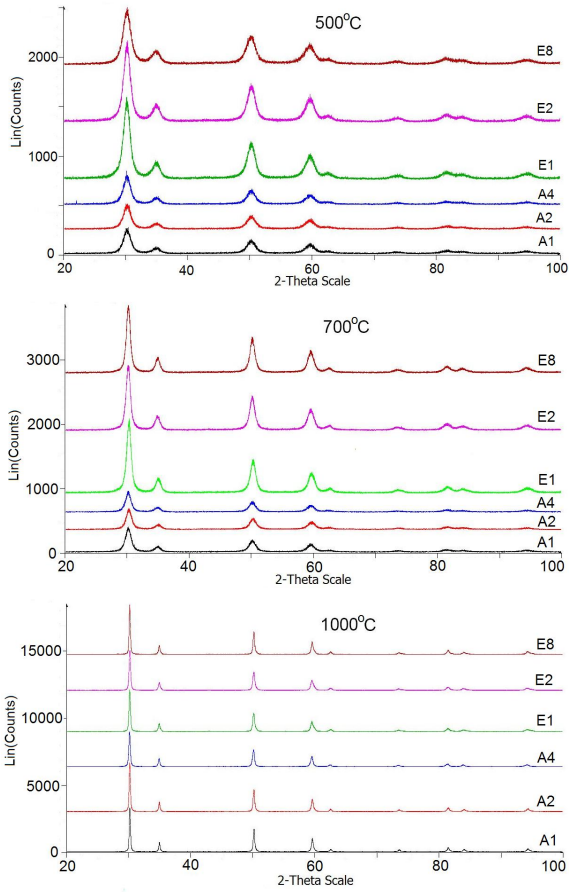

Figure 3. The X-ray diffraction spectra size of the samples calcined at 500, 700, and 1000^{0}C.

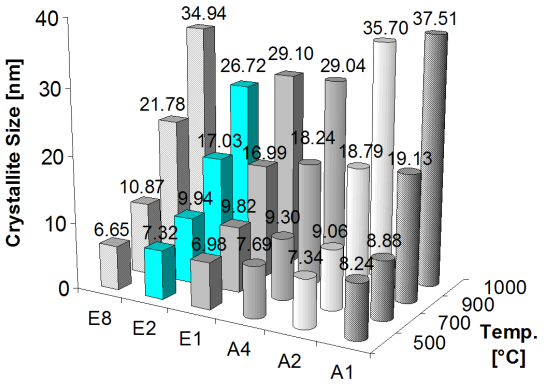

Figure 4. The mean crystallite size of the samples determined by XRD.

A comparison of particle size evaluated from XRD analysis and specific surface area measurements shows that the particles are less agglomerated at low temperatures. The mean particles and agglomerates sizes increase by increasing the calcination temperature. In addition, it can be seen that the specific surface area of the calcined powders regularly decreases when the calcination temperature goes up and the crystallite size of the powders increases. This strengthens the tendency of the particles to form a dense structure in the agglomerate and hence the specific surface area decreases. The calcination temperature and the duration of calcination affect both crystallite size and specific surface area of the powders. The results are comparable with the results obtained by other researchers [2,3,4,9]. Also, the calculated mean crystallites size is smaller than the calculated mean particles size, which is similar to the results obtained by Widoniak et al. [8].

The TEM images confirm the presence in powders of the agglomerates at high temperatures. At 500^0C the nanoparticles are relatively regular, rounded shapes, less agglomerated with a narrow size distribution (Figure 6).

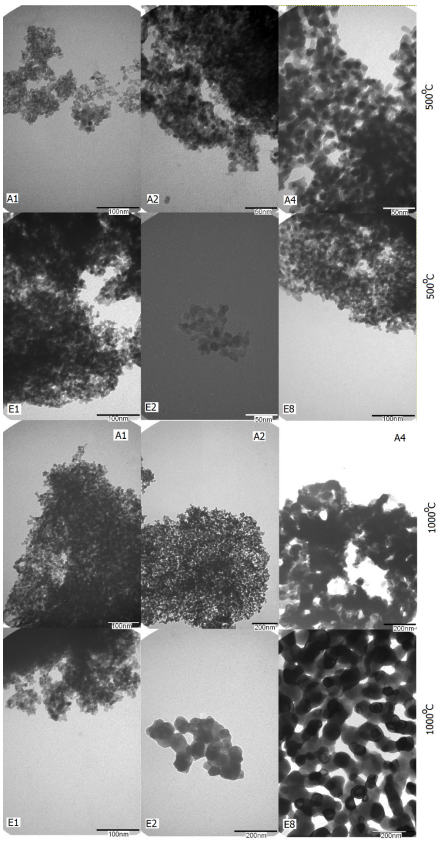

Figure 5. TEM images for the samples calcined at 500 and 1000^0C.

The mean particle size of the samples calcined at 500^0C is between 9 and 14 nm. The powder calcined at 1000^0C showed a partial sintering of the primary crystallites. This result is also observed during the synthesis of YSZ by a combustion process [14] or by a modified Pechini method [15], while the particle size measured for the samples calcined at 1000^0C is between 10 and 60 nm.

As it can be observed from the XRD measurements, the obtained crystallite sizes (6 nm at 500^0C and 37nm at 1000^0C, respectively) are smaller than the mean particle size obtained from the specific surface area measurements (10 nm at 500^0C and 150 nm at 1000^0C). The obtained mean particle sizes from the TEM micrographs (10 nm at 500^0C and 60 nm at 1000^0C, respectively) are more close to the crystallite sizes determined from the XRD. Similar results were found in [8], where the crystallites sizes are much smaller than the particles size and also much higher specific areas than the particle sizes due to the nanoparticles aggregation.

CONCLUSIONS

The influence of the process parameters on the properties of nanoparticles produced with a new sol-gel process using sucrose and pectin in place of conventional organic precursors has been investigated. Compared with the conventional sol-gel method, this method also allows the production of 8mol% YSZ powders at a relatively low temperature with good stoichiometric control, high quality of the produced nanoparticles and high degree of crystallization. The obtained powders using different mass ratio of sucrose and pectin and different calcination temperatures are comparable with the powders obtained through other sol-gel methods using different organic precursors. Comparisons can be made from different points of view, e.g. behavior under calcination; crystallite and particle size; specific surface areas and total pore volume.

High specific surface areas, up to ~100 m^2/g, were obtained by the modified sol-gel method and the calculated particle sizes correspond to 10 nm. The specific surface area is inversely proportional to particle diameter. Pore volumes, specific surface area, mean pore diameter and BJH pore diameter are correlated to each other.

The E set, was found to yield cubic yttria stabilized zirconia with a larger crystallite size as indicated by less noise and smaller peak width at low temperatures (500^0C). The calcination temperature was responsible for the higher crystallization quality observable from the XRD measurement (higher and sharper peaks). C. Laberty-Robert et al. [3] obtained tetragonal 8YSZ at temperatures below 600^0C and they also concluded that the calcination temperature influence the crystallization degree of the powders.

The estimated particle size showed a slightly decreasing trend with the decrease in the sucrose/pectin mass ratio concentration though the preparation condition was identical for all the samples. C. Laberty-Robert et al. [9] found

also that the organic precursor ratio (citric acid and ethylene glycol) and the ratio between the citric acid and metal ions does not influence much the particle sizes of the final powders. Additional studies to investigate the viscosity of the gels are required. The possibility of controlling the particle sizes by adding different surfactants to the initial solutions to obtain a colloidal suspension might also be worth of investigating.

EXPERIMENTAL SECTION

Preparation techniques

$ZrCl_4$ (Sigma-Aldrich, technical purity) and $Y(NO_3)_3 \cdot 6H_2O$ (Sigma-Aldrich, 99.9% purity) were used as raw materials at the molar ratios required to obtain 8YSZ (ZrO_2 doped with 8 mol% Y_2O_3). Two sets of samples labeled A and E, containing the sucrose/pectin mass ratios shown in Table 1 were used in order to study the effect of the amounts and proportions of the organic precursors on the process and the product particles.

Table 1. Sucrose/Pectin mass ratio used in experiments.

	A1	A2	A4	E1	E2	E8
Sucrose	100	100	100	100	100	100
Pectin	2	4	8	0.25	0.5	0.75

The flow chart for the synthesis of the 8YSZ compound powders is shown in Scheme 1. Aqueous solutions of the two salts were stirred on a warming plate at 90–100^{0}C in order to mix the solution uniformly. The sucrose/pectin solution was added gradually into the aqueous solutions under stirring until transparent colloidal suspensions were obtained. The transparent sol continuously transformed into wet gel and then into dried gel under heating. Finally, the obtained gels were calcined at different temperatures: 500, 700 and 1000^{0}C to form white 8 mol% YSZ compound nanoparticles. Each gel sample was calcined, in air, at a heating rate of 100^{0}C/h. The calcination temperature diagram, was designed in accordance with the results of the TG/TDA experiments discussed above The plateaus were as follows:

– 500◦C: 1 hr at 200^{0}C, 2 hrs at 400^{0}C and 6 hrs at 500^{0}C
– 700◦C: 1 hr at 200^{0}C, 2 hrs at 400^{0}C and 4 hrs at 700^{0}C
– 900◦C: 1 hr at 200^{0}C, 2 hrs at 400^{0}C, 3 hrs at 600^{0}C and 3 hrs at 900^{0}C
– 1000◦C: 1 hr at 200^{0}C, 2 hrs at 400^{0}C, 3 hrs at 600^{0}C and 2 hrs at 1000^{0}C.

This mechanism, and the role played by sucrose and pectin in the formation of YSZ powders, is discussed in more detail in reference [10]. The addition of sucrose and pectin to the solution of the metal cations forms a polymer matrix in which the Zr^{4+} and Y^{3+} cations are distributed through the polymeric network structure. Sucrose, which is always in excess, acts as a strong chelating

agent and as a pattern material. The sucrose solution contains NO^{3-} ions, which helps to hydrolyze the sucrose molecule into glucose and fructose, and afterwards oxidized to gluconic acid (GA) or polyhydroxyl acid. GA contains carboxilyc acid groups and hydroxyl groups which can participate in the complexation of metal ions and may form branched polymer with pectin. Pectin chains form long layers and sucrose molecules may bind between this layers. In the present process, metallic ions are bound by the sucrose molecule and the resulting complex molecule is trapped between pectin layers. During calcination this polymeric metal ion complex is decomposed into CO_2 and H_2O and a large amount of heat is generated preventing agglomeration by ensuring that the mixture remains porous.

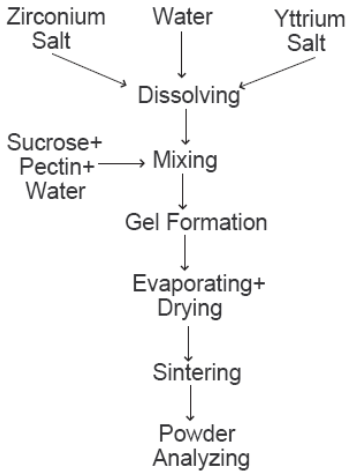

Scheme 1. Flow chart for 8YSZ preparation technique.

Analysis techniques

Thermo-gravimetry and differential thermal analysis (TG/DTA) curves were recoreded with a thermal analyzer Derivatograph Q 1500 (MOM Hungary) up to 1000^0C, in air, at a heating rate of 10^0C/min, using Al_2O_3 as reference. Apart from giving information about the physical and chemical processes taking place during calcination, the TA analyses were used for determining the optimal calcination temperature scheme (the levels and durations of the temperature plateaus described above) to allow the processes, such as dewatering, zirconia formation and solid solution formation to go to completion before proceeding with raising the temperature.

The BET specific surface area SBET and pore volume (V_P) distribution were measured by nitrogen physisorbtion using an Gemini 2380 analyzer from Micromeritics Co.Ltd. The pore size distribution was calculated from the

adsorbtion branch of the isotherms, based on the BJH method. The BJH pore diameter (r_p) was calculated as $4V_p/S_{BJH}$ [11]. All the final powders were degassed at 200^0C for 3h under vacuum before analysis.

X-ray diffraction patterns were generated using a Brucker D-8 Advance X-ray diffractometer with CuKα1 radiation in the 2θ range of 20-100 Å. The crystallite sizes were calculated from the XRD spectra using the Scherrer formula $D = \lambda/(\beta \cos\theta)$, where D is the crystallite size, λ is the wavelength (0.15406 nm), β is the Full Width at Half Maximum (FWHM) and θ is the diffraction angle.

The morphologies of the powders were examined by TEM (transmission electron microscopy) using a JEOL-JEM-1011 transmission microscope. From the samples dispersed in water under stirring, one drop was taken and deposited on a copper grid (Agar G2400C, 400 Square Mesh, copper 3.05mm). The grids were previously covered with an organic layer of Formvar powder (Agar Scientific LTD, Essex) dissolved in chloroform followed by carbon deposition process under vacuum (Agar Turbo carbon coater, Model 208C) and a glow discharge.

ACKNOWLEDGMENTS

This work was funded by the NFR (Norwegian Research Council) and Prototech A.S., Bergen, Norway made laboratory facilities available. Also, the authors are acknowledging the Laboratory for Electron Microscopy, University of Bergen, Norway for helping with all the micrographs.

REFERENCES

1. C.J. Brinker, G.W. Scherer, Sol-gel science: the physics and chemistry of sol-gel processing, Academic Press, New York, **1990**.
2. Y. Zhang, A. Li, Z. Yan, G.Xy, C. Liao, C. Yan, *Journal of Solid State Chemistry*, **2003**, *171*, 434.
3. C. Laberty-Robert, F. Ansart, C. Deloget, M. Gaudon, A. Rousset, *Materials Research Bulletin,* **2001**, *36*, 2083.
4. X. Wang, M. Wang, H. Song, B. Ding, *Materials Letters*, **2006**, *60*, *2261.*
5. J.S. Lian, X.Y. Zhang, H.P. Zhang, Z.H. Zhang, J. Zhang, *Materials Letters* **2004**, *58*, 1183.
6. A. Mali, A. Ataie, *Ceramics International,* **2004**, *30,* 1979.
7. K.Y. Jung, S. B. Park, M. Anpo, *Journal of Photochemistry and Photobiology A: Chemistry,* **2005**, *170,* 247.
8. J. Widoniak, S. Eiden-Assmann, G. Maret, C*olloids and Surfaces A: Physicochem. Eng. Aspects,* **2005**, *270–271,* 329.

9. C. Laberty-Robert, F. Ansart, S. Castillo, G. Richard, *Solid State Sciences,* **2002**, *4*, 1053.
10. C. Suciu, A.C. Hoffmann, A. Vik, F. Goga, *Chemical Engineering Journal,* **2008***,138*, 608.
11. E.P. Barrett, L.G. Joyner, P.H. Halenda, *Journal of the American Chemical Society,* **1951**, *73*, 373.
12. M. El-sayed Ali, Omar A. Abdelal, Ahmed A. Hassan, *Solid State Ionics*, **2007**, *178*, 1463.
13. H.M. Rietveld, *Journal of Applied Crystallography*, **1969**, *2*, 65.
14. K.R. Venkatachari, D. Huang, S.P. Ostrander, W.A. Sculze, G.C. Stangle, *Journal of Materials Research*, **1995**, *10*, 748.
15. C.L. Robert, F. Ansart, C. Deloget, M. Gaudon, A. Rousset, *Ceramics International,* **2003**, *29*, 151.